Journal of Optimization Theory and Applications (2021) 191:393–414
https://doi.org/10.1007/s10957-020-01735-5

Maximum Conditional Probability Stochastic Controller for Linear Systems with Additive Cauchy Noises

Nati Twito[1] · **Moshe Idan**[1] · **Jason L. Speyer**[2]

Received: 5 August 2019 / Accepted: 30 July 2020 / Published online: 7 August 2020

Abstract

Motivated by the sliding mode control approach, a stochastic controller design methodology is developed for discrete-time, vector-state linear systems with additive Cauchy-distributed noises, scalar control inputs, and scalar measurements. The control law exploits the recently derived characteristic function of the conditional probability density function of the system state given the measurements. This result is used to derive the characteristic function of the conditional probability density function of the sliding variable, utilized in the design of the stochastic controller. The incentive for the proposed approach is mainly the high numerical complexity of the currently available method for such systems, that is based on the optimal predictive control paradigm. The performance of the proposed controller is evaluated numerically and compared to the alternative Cauchy controller and a controller based on the Gaussian assumption. A fundamental difference between controllers based on the Cauchy and Gaussian assumptions is the superior response of Cauchy controllers to noise outliers. The newly proposed Cauchy controller exhibits similar performance to the optimal predictive controller, while requiring significantly lower computational effort.

Keywords Stochastic control · Optimal controller synthesis for systems with uncertainties · Heavy tailed distributions

Mathematics Subject Classification 93E20

✉ Moshe Idan
moshe.idan@technion.ac.il

Nati Twito
nati0605@gmail.com

Jason L. Speyer
speyer@g.ucla.edu

[1] Technion - Israel Institute of Technology, Haifa, Israel

[2] Mechanical and Aerospace Engineering, University of California, Los Angeles, CA, USA

1 Introduction

The majority of stochastic control methodologies assume that the dynamical system is driven by additive Gaussian process and measurement noises [1,2]. Many solutions to the control problem for linear systems with Gaussian noise distributions can be readily found in the literature, e.g., the commonly used Linear Quadratic Gaussian (LQG), Linear Exponential Gaussian (LEG), $\mathcal{H}_2$ and $\mathcal{H}_\infty$, and more [1–3]. However, the Gaussian assumption is incompatible with systems forced by heavy-tail distributed noises exhibiting significant measurement and process noise outliers caused by, e.g., radar and sonar sensors, atmospheric disturbances and air turbulence, and more [4,5]. Using light-tailed Gaussian approximations for such cases showed significant performance degradation in the presence of outliers [6,7].

Recent studies showed that the heavy-tailed Cauchy distribution is an attractive candidate, since it better represents process and measurement noise outliers in both estimation and control design [6–10]. In those studies, the heavy-tailed Cauchy densities were directly employed in the design process. Although no physical phenomenon is explicitly Cauchy distributed, since its tails over bound other realistic densities, estimators and controllers that are based on the Cauchy probability density function (pdf) are hypothesized to be robust to unknown realistic physical densities. We refer to robustness in the statistical sense [11], meaning that the estimator achieves adequate performance when faced with outliers or unexplained events, and where these events may arise either as large measurement errors, large process deviations, or due to misspecification of the dynamic model.

The Cauchy distribution is challenging, because its unconditional first moment is not well defined and its unconditional higher moments are infinite. However, for estimation, it was shown that the conditional pdf of the state given the measurement history has finite conditional first and second moments, yielding the conditional minimum variance Cauchy estimator [8–10].

Because of the undefined second moments of the noise signals, when posing the control problem for such systems, commonly used cost criteria (e.g., the quadratic cost of LQG) are not properly defined, i.e., their unconditional expectation is not finite. A cost criterion, whose functional form is similar to that of the Cauchy pdf, is properly defined. Moreover, the conditional expectation of this cost criterion can be obtained in closed-form and used in the controller design. In [8–10], it was shown that the time propagated conditional pdf of the system state given the measurement history is a nonlinear function of the measurement sequence. This, clearly, complicates the control design task, since the controller becomes a nonlinear function of the measurements. Nonetheless, the conditional pdf was incorporated in an optimal predictive control (OPC[1]) design setting that uses the above mentioned computable cost criterion, which is both well defined and finite [6,7]. The main drawback of those predictive controllers is their high complexity and computational load. This is caused by the complex form of the cost and the solution to the nonlinear, non-convex optimization required to determine numerically the optimal control sequence. The goal of the current work is

[1] In [7], this methodology was referred to as Cauchy-MPC.

to suggest a controller, that significantly reduces the computational burden without affecting its performance.

The controller design presented in the current study is motivated by the sliding mode control (SMC) method [12,13]. In SMC, the desired closed-loop dynamic characteristics of the system are specified by defining a sliding variable. Nullifying the sliding variable, thus driving the system into a sliding mode, guarantees the desired performance. The control method ensures that a system with bounded disturbances will attain the sliding mode in a finite time. However, when addressing systems with unbounded or stochastic disturbances, sliding mode behavior cannot be obtained even when the time frame is not limited. As an alternative, it was proposed regulating the sliding variable to within a predefined bound around the sliding mode [14–16]. This method was successfully applied for systems with Gaussian noises. Design of this stochastic controller relies on the second moment of the controlled-system state. Since those moments are not finite in the Cauchy noise case, the method proposed in [15] is modified and expanded to address the heavy-tailed noise case considered here.

This methodology applied to scalar-state systems with Cauchy noises was presented in [17]. The controller design is based on the conditional pdf of the state given the measurement history that is available only for the scalar case [8] and hence cannot be extended to the vector-state case. Still, the scalar-state case provides important insights. Therefore, those results are presented here for completeness. The scalar-state results are generalized to address vector-state, single-input single-output linear systems. This generalization accounts for the fact that the cost criterion must be constructed from the characteristic function (cf) of the conditional pdf rather than directly from the conditional pdf, which is unavailable for the vector case [10]. The results can be readily extended to multi-output systems, affecting only the computation of the cf of the conditional pdf which can be performed using the algorithm presented in [10].

This paper is organized as follows. The control problem, addressed in this study, is formulated in Sect. 2, followed by the solution concept in Sect. 3. A detailed derivation of the proposed control method is then presented in Sect. 4, first for a scalar-state and then for a vector-state linear system. The resulting controller is evaluated through numerical simulations and contrasted to alternative solutions in Sect. 5. The paper is concluded in Sect. 6.

2 Problem Formulation

We consider a linear, discrete-time stochastic system

$$x_{k+1} = \Phi x_k + \Lambda u_k + \Gamma w_k, \tag{1a}$$

$$z_k = H x_k + v_k, \tag{1b}$$

where $x_k \in \mathbb{R}^n$ is the system state, u_k is a scalar control signal used to regulate x_k, z_k is a scalar linear measurement, and k is the time index. The matrices Φ, H, Λ and Γ with appropriate dimensions are assumed to be known. The scalar process noise w_k and measurement noise v_k are assumed to be white, independent of each other and the initial state x_1, Cauchy-distributed random processes with pdf-s given by

$$f_{W_k}(w_k) = \frac{\beta/\pi}{w_k^2 + \beta^2}, \quad \beta > 0, \tag{2a}$$

$$f_{V_k}(v_k) = \frac{\gamma/\pi}{v_k^2 + \gamma^2}, \quad \gamma > 0. \tag{2b}$$

Their characteristic functions are given by

$$\phi_{W_k}(\bar{\nu}) = e^{-\beta|\bar{\nu}|}, \tag{3a}$$

$$\phi_{V_k}(\bar{\nu}) = e^{-\gamma|\bar{\nu}|}, \tag{3b}$$

where $\bar{\nu}$ is the scalar spectral variable. The initial condition is also chosen to be Cauchy-distributed, consisting of n random variables that are assumed to be independent of each other. Hence, the joint pdf of the initial conditions is given by

$$f_{X_1}(x_1) = \prod_{i=1}^{n} \frac{\alpha_i/\pi}{[x_1(i) - \bar{x}_1(i)]^2 + \alpha_i^2}, \quad \alpha_i > 0, \tag{4}$$

where $x_1(i)$ are elements of x_1 and $\bar{x}_1(i)$ are elements of the vector $\bar{x}_1$ of medians. Its characteristic function is given by

$$\phi_{X_1}(\nu) = \prod_{i=1}^{n} e^{-\alpha_i|\nu_i| + j\bar{x}_1(i)\nu_i}, \quad \alpha_i > 0, \tag{5}$$

where $\nu \in \mathbb{R}^n$ is the vector-valued spectral variable with ν_i being an element of ν.

The goal is to design an output feedback controller, i.e., u_k, being a function of the measurement history $y_k = \{z_1, \ldots, z_k\}$, to regulate the state x_k. The tracking problem can be addressed using a similar method.

3 Stochastic Control Design Concept

The challenge in addressing the control design problem of linear systems with Cauchy-distributed noises stems from the fact that notions like certainty equivalence do not hold in this case. Specifically, it was shown in [8–10] that the minimum conditional variance estimator of such systems is nonlinear in the measurement history. Moreover, the unconditional moments of the system state are either not defined or infinite. Thus, the commonly used control design criteria have to be modified when addressing such system, as was suggested in [6,7]. The resulting controller was shown to be a highly nonlinear function of the measurement history, entailing high computational load. In order to address the computational challenge of the known solutions [6,7], this study suggests a design methodology that is motivated by the SMC method that addresses mainly systems with bounded uncertainties and noises [12,13], and is extended to stochastic systems [14–16]. We first briefly review those results.

Consider the linear multivariate discrete-time system defined in (1). First, assuming full state information and bounded disturbance w_k for all k, the task is to regulate x_k. In SMC, we define a sliding variable

$$s_k = cx_k, \tag{6}$$

where for a scalar control input u_k, $s_k : \mathbb{R}^n \to \mathbb{R}$, and $c \in \mathbb{R}^{1\times n}$ is a design parameter such that $c\Lambda \neq 0$. The sliding surface is defined as

$$\mathcal{S} = \{x_k | \, s_k = cx_k = 0\}. \tag{7}$$

When $\mathcal{S}$ is attained, the system is said to be in a sliding mode. c is chosen such that when the system is in the sliding mode, it complies with the desired closed-loop dynamics requirements (see [12,13] for details.) Specifically, when $w_k = 0$, choosing the control signal to be

$$u_k = -\left(c\Lambda\right)^{-1} c\Phi x_k \tag{8}$$

yields

$$s_{k+1} = cx_{k+1} = c\Phi x_k + c\Lambda u_k = 0. \tag{9}$$

Hence, the sliding mode is reached in one step, and its closed-loop dynamics is given by

$$x_{k+1} = \Phi x_k + \Lambda u_k = \left(\Phi - \Lambda(c\Lambda)^{-1} c\Phi\right) x_k = \tilde{\Phi} x_k. \tag{10}$$

The vector c is chosen such that the closed-loop transition matrix $\tilde{\Phi}$ is Schur, i.e., its eigenvalues are inside the unit circle and provide the desired closed-loop dynamic characteristics. Controllability of the pair (Φ, Λ) and observability of (c, Φ) are sufficient conditions to comply with those design requirements. There are additional methods for choosing the vector c, e.g., embedding optimal control tools and more, that can be found in the literature [12].

In the presence of bounded noises and uncertainties, the discrete sliding mode control signal is set to be

$$u_k = u_{(dis)_k} + u_{(eq)_k} = -\rho \, \text{sign}(s_k) - \left(c\Lambda\right)^{-1} c\Phi x_k. \tag{11}$$

$u_{(dis)_k}$ is a discontinuous control signal designed to drive the system into a sliding mode in a finite time, while $u_{(eq)_k}$ ensures that the system remains on $\mathcal{S}$. The parameter ρ depends on the bound of the disturbance and regulates the finite time required for the system to reach the sliding mode. SMC solutions are available also for the output feedback setting, where only the measurement z_k is available [12].

When addressing stochastic systems with unbounded noises, it is not feasible to drive the system into a sliding mode or maintain it over time: the stochastic signal will continuously divert the system from the sliding surface. Hence, to apply the SMC ideas for such systems, concepts like the sliding surface and finite time convergence have to be modified to yield a stochastic version of the SMC approach. Such ideas were proposed in [14–16], where the disturbances were assumed to be Gaussian white noises.

The main idea in these studies is to construct an output feedback control law u_k, such that the system (1) is driven to a vicinity of the sliding surface $\mathcal{S}$ of (7) with a given probability and is kept in this region over time. Specifically, for a bound $L > 0$ and $0 < \varepsilon < 1$, the goal is to attain

$$P\left(|s_k| < L\right) = 1 - \varepsilon \quad \text{a.s.} \quad \forall k > N \tag{12}$$

for some integer N. In [15], it is shown that for the Gaussian case, by incorporating a Kalman filter estimator, a stochastic controller can be designed to ensure (12), where, for a given ε, the bound L can be determined analytically as a function of the measurement-independent second moment of the state estimation error.

This is not the case for systems with Cauchy-distributed noises, for which the conditional estimator and the estimation error variance are highly nonlinear functions of the measurement history [8–10]. Moreover, due to the heavy-tail characteristics of the process noise, the time propagated conditional pdf does not have a well-defined first moment, i.e., there is no time propagated estimate of the state, and has an infinite second moment needed to apply the methodology in [15]. Hence, a modified approach is proposed here to address systems with Cauchy-distributed noises.

Therefore, instead of designing a controller for a prescribed probability $(1 - \varepsilon)$ in (12) and computing the bound L for it as suggested in [15], for the Cauchy case it is proposed to set the bound L a priori and determine the control signal u_k such that the *a priori* conditional probability of the sliding variable s_{k+1} to be in the band $\pm L$ around zero is maximized, i.e.,

$$u_k^* = \arg\max_{u_k} P\left(|s_{k+1}| < L | \, y_k\right). \tag{13}$$

The above probability is computed using the conditional pdf of the sliding variable s_{k+1} given the measurement history that can be determined from the conditional pdf of the state x_{k+1} at time step $k+1$ given y_k, $f_{X_{k+1}|Y_k}(x_{k+1}|y_k)$, or its characteristic function. Fortunately, this pdf or its characteristic functions were derived analytically when addressing the Cauchy estimation problem and hence can be readily used to compute u_k^* in (13). This proposed controller will be referred to as the maximum-conditional-probability-controller (MCPC).

For scalar-state systems, $f_{X_{k+1}|Y_k}(x_{k+1}|y_k)$ is computed analytically in closed form in [8] and is used to design the MCPC. In the vector-state case, only the characteristic function of $f_{X_{k+1}|Y_k}(x_{k+1}|y_k)$ could be computed analytically [10]. Consequently, the MCPC for vector-state systems will be derived while using those characteristic functions, as is detailed in the next section.

4 Maximum Conditional Probability Controller

As discussed in the previous section, the control synthesis relies on the conditional pdf of the state x_{k+1} given the measurement history y_k. For scalar-state systems described in (1) with $n = 1$, this pdf is expressed as a recursive and analytic function of the measurement history and system parameters [8], and can be used to derive the MCPC

in the most natural way, as is presented in the first subsection below. For vector-state systems, only the characteristic function of this conditional pdf, also expressed as a recursive and analytic function of the measurement history and the system parameters, is derived in [10]. Therefore, the optimization in (13) will have to be first re-cast in the characteristic function formulation before being solved for the vector-state case. In this section, for clarity and completeness of the presentation, we recap first the scalar-state case that was originally presented in [17]. Then, we will address the vector-state case, presented in the last subsection below.

4.1 Scalar-State MCPC

In this subsection, we address the scalar-state case. Since the state is scalar, without loss of generality, we set $\Lambda = \Gamma = 1$ in (1a) and choose the sliding variable of (6) to be equal to the system state, i.e., $c = 1$. Moreover, we first present the controller derivation while using the pdf of the time propagated state x_{k+1} given the measurement history y_k, followed by an alternative derivation that utilized the characteristic function of that pdf. The latter is presented as the background for the vector-state case, where only the characteristic function is known in closed analytical form.

4.1.1 Pdf Derivation

In [8], it was shown that $f_{X_{k+1}|Y_k}(x_{k+1}|y_k)$ can be expressed in a closed analytical form as

$$f_{X_{k+1}|Y_k}(x_{k+1}|y_k) = \sum_{i=1}^{k+1} \frac{a_i(k+1|k)x_{k+1} + b_i(k+1|k)}{(x_{k+1} - \sigma_i(k+1|k))^2 + \omega_i^2(k+1|k)}. \tag{14}$$

In the above, the $(k+1|k)$ notation implies that the respective parameters appear in the conditional pdf of the state at time step $k+1$ given the measurement history up to time step k. Similar notation will be used in the remainder of the text. Recursive, closed-form expressions for all the parameters in (14), that are nonlinear functions of the system parameters and the measurement history, can be found in reference [8].

Following the rationale presented in the previous section and expressed implicitly in Eq. (13), the optimal control signal u_k is determined by maximizing the cost function

$$J_k^* = \max_{u_k} \int_{-L}^{L} f_{X_{k+1}|Y_k}(x_{k+1}|y_k)\, dx_{k+1}, \tag{15}$$

where the pdf $f_{X_{k+1}|Y_k}(x_{k+1}|y_k)$ is a nonlinear function of the control signal u_k, i.e., the parameters $\sigma_i(k+1|k)$ in (14) are affine in u_k [8]. Due to the affine relation of x_{k+1} on the input u_k in (1a), a variation in u_k shifts $f_{X_{k+1}|Y_k}(x_{k+1}|y_k)$ along the x_{k+1}-axis by the value of u_k compared to $f_{X_{k+1}|Y_k}(x_{k+1}|y_k)$ computed when $u_k = 0$. Therefore, the cost function in (15) can be expressed alternatively as

$$J_k^* = \max_{u_k} \int_{-L-u_k}^{L-u_k} f_{X_{k+1}|Y_k}^{u_k=0}(x_{k+1}|y_k)\, dx_{k+1}, \tag{16}$$

where $f_{X_{k+1}|Y_k}^{u_k=0}(x_{k+1}|y_k)$ is the time-propagated pdf of x_{k+1} given the measurement history y_k when assuming that $u_k = 0$. Its analytical form is identical to that given in (14) with appropriate changes in pdf parameters $\sigma_i(k+1|k)$. The advantage of using the cost in (16) is that $f_{X_{k+1}|Y_k}^{u_k=0}(x_{k+1}|y_k)$ has to be computed only for $u_k = 0$ and not repeatedly for every candidate u_k when solving the maximization problem of (15). Hence, the form in (16) will be used in the sequel to determine numerically the optimal cost J_k^* to yield the optimal control signal given by

$$u_k^* = \arg\max_{u_k} \int_{-L-u_k}^{L-u_k} f_{X_{k+1}|Y_k}^{u_k=0}(x_{k+1}|y_k)\, dx_{k+1}. \tag{17}$$

Using the explicit form of $f_{X_{k+1}|Y_k}^{u_k=0}(x_{k+1}|y_k)$ given in (14), the integral of the control performance cost in (16) can be solved analytically [18] to yield

$$J_k(u_k) = \int_{-L-u_k}^{L-u_k} f_{X_{k+1}|Y_k}^{u_k=0}(x_{k+1}|y_k)\, dx_{k+1} = \sum_{i=1}^{k+1} \left\{ \frac{a_i}{2} \ln \frac{(L-u_k-\sigma_i)^2+\omega_i^2}{(-L-u_k-\sigma_i)^2+\omega_i^2} + \frac{a_i\sigma_i + b_i}{\omega_i} \left[\arctan\left(\frac{L-u_k-\sigma_i}{\omega_i}\right) - \arctan\left(\frac{-L-u_k-\sigma_i}{\omega_i}\right) \right] \right\}. \tag{18}$$

In the above, for simplicity, the time indices $(k+1|k)$ were removed from the pdf parameters.

The cost in (18) is a highly nonlinear function of the optimization parameter u_k. Moreover, it was observed empirically that it is not convex and may have several local maxima. Consequently, a global maximum of $J_k(u_k)$ cannot be determined analytically. Therefore, the maximization of $J_k(u_k)$ is performed using standard numerical optimization tools available, e.g., in MATLAB. The gradient of (18) with respect to u_k can be easily computed as the difference between the values of the integrand given in (14) evaluated at the integration limits. However, using a gradient-search method, computing the gradient from its closed-form expression is numerically expensive and leads to longer optimization times compared to non-gradient-based methods. Hence, we use a MATLAB function that implements the Nelder–Mead simplex algorithm: an enormously popular direct search (derivative-free) method for multidimensional unconstrained maximization [19].

Since the numerical search normally finds only a local extremum, its result depends on the initial guess provided by the user. We have observed that in most cases the integrand $f_{X_{k+1}|Y_k}^{u_k=0}(x_{k+1}|y_k)$ in (18) has at most two distinct peaks: one around zero,

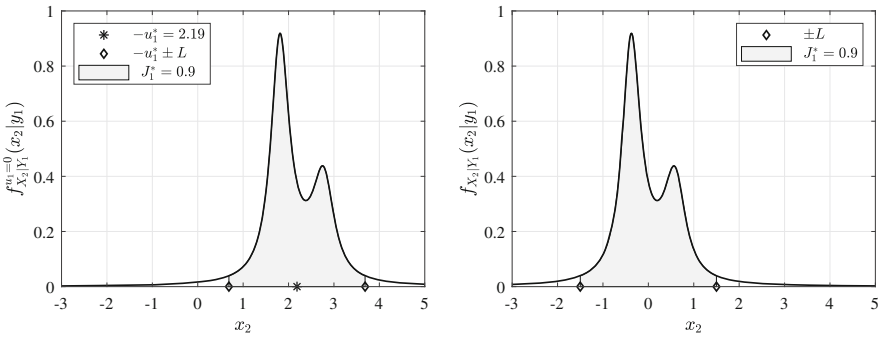

(a) $f^{u_1=0}_{X_2|Y_1}(x_2|y_1)$, J_1^* of (16) and u_1^*. **(b)** $f_{X_2|Y_1}(x_2|y_1)$ and J_1^* of (15).

Fig. 1 $f^{u_1=0}_{X_2|Y_1}(x_2|y_1)$, $f_{X_2|Y_1}(x_2|y_1)$, J_1^* and u_1^*

and one around a scaled value of an outlier measurement, i.e., $z(k)\Phi/H$.[2] Normally, the local maxima will be found in the vicinity of those peaks. Hence, the numerical search is performed twice, starting from initial guesses of zero and $z(k)\Phi/H$, and u_k^* is chosen as the one that yields a higher value of $J_k(u_k^*)$. This u_k^* is used as an input to the system and to compute the actual time propagated $f_{X_{k+1}|Y_k}(x_{k+1}|y_k)$. In the cases that (18) has more than two peaks, a phenomenon that is both rare and does not normally persists for more than one step, the search will converge to a temporary local maximum, and will revert to the global maximum once the third peak diminishes.

To demonstrate the shifting relation between the two time-propagated pdf-s mentioned above together with the maximization process, we consider a sample system with parameters $\Phi = 0.9$, $H = 1$, $\bar{x}_1 = 2$, $\alpha = 0.02$, $\beta = 0.2$, and $\gamma = 0.1$. At time $k = 1$, the initial state was drawn from its Cauchy distribution to be $x_1 = 2.014$, while the measurement at this initial time instant was drawn to be $z_1 = 3.1$. The time propagated $f^{u_1=0}_{X_2|Y_1}(x_2|y_1)$ computed for $u_1 = 0$ is depicted in Fig. 1a. Choosing $L = 1.5$ and solving (16), it was determined numerically that $J_1^* = 0.9$. It is depicted in Fig. 1a by the gray area. This optimal cost was obtained for $u_1^* = -2.19$, whose negative values are also shown in this figure. Finally, $f_{X_2|Y_1}(x_2|y_1)$ computed with the optimal control signal is depicted in Fig. 1b. Since $u_1^* = -2.19$ is negative, it clearly shows that the latter pdf is shifted by 2.19 to the left compared to $f^{u_1=0}_{X_2|Y_1}(x_2|y_1)$ in Fig. 1a. This example also demonstrated the two-peak occurrence discussed in the previous paragraph.

[2] It was shown in [8] that during a measurement update at time step k, a new term is generated in the sum of (14) that is centered at $\sigma_{k+1}(k|k) = z(k)/H$. The center of this terms is moved to $\sigma_{k+1}(k+1|k) = z(k)\Phi/H$ when propagated to time step $k+1$. Hence, if $z(k)\Phi/H$ is large, it will produce a secondary peak in $f^{u_k=0}_{X_{k+1}|Y_k}(x_{k+1}|y_k)$.

4.1.2 Characteristic Function Implementation

An alternative approach for the optimal control strategy discussed in this work is to utilize the characteristic function of the un-normalized conditional pdf[3] (cf-ucpdf) of the state x_{k+1} given the measurement history y_k derived analytically for the Cauchy noise case in [9]. This approach will be in particular useful when addressing, in the next subsection, vector-state systems, for which an analytical expression of the conditional pdf is not known [10]. The time-propagated cf-ucpdf mentioned above is expressed as

$$\bar{\phi}_{X_{k+1}|Y_k}(\nu) = \sum_{i=1}^{k+1} (c_i(k+1|k) + j d_i(k+1|k)\ \mathrm{sign}(\nu)) \times e^{-\omega_i(k+1|k)|\nu| + j\sigma_i(k+1|k)\nu}, \tag{19}$$

where j is the pure imaginary number. Recursive, closed-form expressions for all the parameters in (19), that are nonlinear functions of the system parameters and the measurement history, can be found in reference [9]. To obtain the characteristic function of the *normalized* conditional pdf, the above characteristic function has to be divided by

$$f_{Y_k}(y_k) = \bar{\phi}_{X_{k+1}|Y_k}(\nu)\big|_{\nu=0} = \sum_{i=1}^{k+1} c_i(k+1|k), \tag{20}$$

to yield

$$\phi_{X_{k+1}|Y_k}(\nu) = \frac{\bar{\phi}_{X_{k+1}|Y_k}(\nu)}{f_{Y_k}(y_k)}. \tag{21}$$

The control performance criterion of (16) can be expressed directly using the characteristic function of the associated pdf [20], i.e.,

$$\begin{aligned} J_k^* &= \max_{u_k} \int_{-L-u_k}^{L-u_k} f_{X_{k+1}|Y_k}^{u_k=0}(x_{k+1}|y_k)\, dx_{k+1} \\ &= \max_{u_k} \frac{1}{\pi} \int_{-\infty}^{\infty} \frac{\sin(L\nu)}{\nu} e^{ju_k\nu} \phi_{X_{k+1}|Y_k}^{u_k=0}(\nu) \mathrm{d}\nu, \end{aligned} \tag{22}$$

where $\phi_{X_{k+1}|Y_k}^{u_k=0}(\nu)$ is the characteristic function of $f_{X_{k+1}|Y_k}^{u_k=0}(x_{k+1}|y_k)$. It should be noted that since those normalization in (21) involves a real and positive parameter $f_{Y_k}(y_k)$, an equivalent cost function can be defined using the un-normalized characteristic function, i.e.,

[3] From Bayes' rule, the un-normalized conditional pdf is the joint pdf of the state and the measurement history, where the normalization factor is the pdf of the measurement history. The propagation of the un-normalized conditional pdf yields an analytic, recursive scheme.

$$\bar{J}_k(u_k) = \frac{1}{\pi}\int_{-\infty}^{\infty} \frac{\sin(L\nu)}{\nu} e^{ju_k\nu}\bar{\phi}^{u_k=0}_{X_{k+1}|Y_k}(\nu)\mathrm{d}\nu, \tag{23}$$

the maximization of which with respect to u_k will yield the same optimal u_k^* as in (22).

The integral in (23) can be solved analytically using the factored form of $\bar{\phi}^{u_k=0}_{X_{k+1}|Y_k}(\nu)$ given in (19). It is expressed as [18]

$$\bar{J}_k(u_k) = \frac{1}{\pi}\sum_{i=1}^{k+1}\left\{\frac{d_i}{2}\ln\frac{(L-u_k-\sigma_i)^2+\omega_i^2}{(-L-u_k-\sigma_i)^2+\omega_i^2} + c_i\left[\arctan\left(\frac{L-u_k-\sigma_i}{\omega_i}\right) - \arctan\left(\frac{-L-u_k-\sigma_i}{\omega_i}\right)\right]\right\}. \tag{24}$$

For simplicity, in (24) the time indices $(k+1|k)$ were removed from the parameters of the characteristic function. Since addressing the same problem, as expected, this result matches the one obtained in (18) with the appropriate relations between the coefficients a_i and b_i in (14) and the coefficients c_i and d_i in (19). Similarly to (18), the optimal control signal that maximizes the cost in (24) is determined numerically using the same method discussed in Sect. 4.1.1. Then, it is used to both drive the system and to determine the time propagated $\bar{\phi}_{X_{k+1}|Y_k}(\nu)$.

4.2 Vector-State MCPC

The proposed controller design scheme involves the sliding variable defined in (6) and the performance criterion in (13), that is determined by solving the maximization problem

$$J_k^* = \max_{u_k}\int_{-L}^{L} f_{S_{k+1}|Y_k}(s_{k+1}|y_k)\,ds_{k+1}. \tag{25}$$

The conditional pdf of the sliding variable, $f_{S_{k+1}|Y_k}(s_{k+1}|y_k)$, can be related to $f_{X_{k+1}|Y_k}(x_{k+1}|y_k)$ [2]. However, only the characteristic function of $f_{X_{k+1}|Y_k}(x_{k+1}|y_k)$ can be obtained in closed form for the multivariate Cauchy case [10]. Therefore, the controller derivation will be performed using the characteristic functions of the random variables. Specifically, as in (22), the integral in (25) can be expressed using the cf of $f_{S_{k+1}|Y_k}(s_{k+1}|y_k)$, $\phi_{S_{k+1}|Y_k}(\eta)$, as [20]

$$J_k = \frac{1}{\pi}\int_{-\infty}^{\infty} \frac{\sin(L\eta)}{\eta}\phi_{S_{k+1}|Y_k}(\eta)\mathrm{d}\eta, \tag{26}$$

where η is the scalar spectral variable.

Evaluating (26) requires the characteristic function $\phi_{S_{k+1}|Y_k}(\eta)$. However, in [10] it is shown only how to determine the characteristic function of the conditional pdf of the state vector, i.e., $\phi_{X_{k+1}|Y_k}(\nu)$, for the vector-state linear system with Cauchy noise

and a vector-valued spectral variable ν. The characteristic function $\phi_{S_{k+1}|Y_k}(\eta)$ can be constructed from $\phi_{X_{k+1}|Y_k}(\nu)$ by using Theorem 1.1.7 in [21], expressed as

$$\phi_{S_{k+1}|Y_k}(\eta) = \phi_{X_{k+1}|Y_k}\left(\eta c^T\right). \tag{27}$$

The relation in (27) is valid for any distribution of the state. For the Cauchy case addressed in [10], the characteristic function of the un-normalized pdf of the state was shown to be a sum of $n_t^{k+1|k}$ terms expressed by

$$\bar{\phi}_{X_{k+1}|Y_k}(\nu) = \sum_{i=1}^{n_t^{k+1|k}} g_i^{k+1|k}\left(y_{gi}^{k+1|k}(\nu)\right) \exp\left(y_{ei}^{k+1|k}(\nu)\right). \tag{28}$$

The superscript notation $k+1|k$ indicates that the respective parameters express the cf at time step $k+1$ given the measurement history up to time step k. The cf-unpdf was considered because it yielded recursive, closed-form expressions for all the functions in (28). $\bar{\phi}_{X_{k+1}|Y_k}(\nu)$ is a function of the systems parameters, measurement history, and the spectral vector variable ν. In particular, the function $y_{ei}^{k+1|k}(\nu)$ is a weighted sum of absolute values and linear terms involving ν, $y_{gi}^{k+1|k}(\nu)$ is a vector whose components are a weighted sum of the sign function involving ν, and $g_i^{k+1|k}\left(y_{gi}^{k+1|k}(\nu)\right)$ is a complex rational function involving $y_{gi}^{k+1|k}(\nu)$. See [10] for details. The cf $\phi_{X_{k+1}|Y_k}(\nu)$ of the normalizated pdf of the state is determined by

$$\phi_{X_{k+1}|Y_k}(\nu) = \frac{\bar{\phi}_{X_{k+1}|Y_k}(\nu)}{\bar{\phi}_{X_{k+1}|Y_k}(\nu)\big|_{\nu\to 0}}. \tag{29}$$

Substituting $\nu = \eta c^T$ into (28), the cf-unpdf of s_{k+1} is determined as

$$\begin{aligned}\bar{\phi}_{S_{k+1}|Y_k}(\eta) = \sum_{i=1}^{n_t^{k|k}} &\left(c_i(k+1|k) + j d_i(k+1|k)\,\mathrm{sign}(\eta)\right) \\ &\times e^{-\omega_i(k+1|k)|\eta| + j\sigma_i(k+1|k)\eta},\end{aligned} \tag{30}$$

where

$$c_i(k+1|k) = \mathrm{Real}\left\{g_i^{k+1|k}\left(y_{gi}^{k+1|k}(c^T)\right)\right\}, \tag{31a}$$

$$d_i(k+1|k) = \mathrm{Im}\left\{g_i^{k+1|k}\left(y_{gi}^{k+1|k}(c^T)\right)\right\}, \tag{31b}$$

$$\omega_i(k+1|k) = -\mathrm{Real}\left\{y_{ei}^{k+1|k}(c^T)\right\}, \tag{31c}$$

$$\sigma_i(k+1|k) = \mathrm{Im}\left\{y_{ei}^{k+1|k}(c^T)\right\}. \tag{31d}$$

The cf of the normalized conditional pdf of s_{k+1} is given by

$$\phi_{S_{k+1}|Y_k}(\eta) = \frac{\bar{\phi}_{S_{k+1}|Y_k}(\eta)}{\bar{\phi}_{S_{k+1}|Y_k}(0)}, \tag{32}$$

where

$$\bar{\phi}_{S_{k+1}|Y_k}(0) = f_{Y_k}(y_k) = \sum_{i=1}^{n_t^{k|k}} c_i(k+1|k) \tag{33}$$

is a positive constant [9]. Since the normalization in (32) involves a real and positive value $f_{Y_k}(y_k)$, an equivalent cost function can be defined using the un-normalized characteristic function of (30), i.e.,

$$\bar{J}_k(u_k) = \frac{1}{\pi}\int_{-\infty}^{\infty} \frac{\sin(L\eta)}{\eta}\bar{\phi}_{S_{k+1}|Y_k}(\eta)\mathrm{d}\eta, \tag{34}$$

the maximization of which with respect to u_k will yield the same optimal u_k^* as in (26).

Due to the affine relation of x_{k+1} on the input u_k in (1a), the cf $\bar{\phi}_{X_{k+1}|Y_k}(\nu)$ can be decomposed as [22]

$$\bar{\phi}_{X_{k+1}|Y_k}(\nu) = \bar{\phi}^{u_k=0}_{X_{k+1}|Y_k}(\nu)\cdot e^{j\left(\Lambda^T\nu\right)u_k}, \tag{35}$$

where $\bar{\phi}^{u_k=0}_{X_{k+1}|Y_k}(\nu)$ is computed assuming $u_k = 0$ and has the same functional form as (28), except its parameters are not a function of u_k, as presented in [10]. Substituting (35) into the un-normalized form of (27), $\bar{\phi}_{S_{k+1}|Y_k}(\eta)$ is expressed as

$$\begin{aligned}\bar{\phi}_{S_{k+1}|Y_k}(\eta) &= \bar{\phi}_{X_{k+1}|Y_k}\left(\eta c^T\right)\\ &= \bar{\phi}^{u_k=0}_{X_{k+1}|Y_k}(\eta c^T)\cdot e^{j\left(\Lambda^T c^T\right)u_k\eta} = \bar{\phi}^{u_k=0}_{S_{k+1}|Y_k}(\eta)\cdot e^{j(c\Lambda)u_k\eta}.\end{aligned} \tag{36}$$

Here,

$$\bar{\phi}^{u_k=0}_{S_{k+1}|Y_k}(\eta) = \bar{\phi}^{u_k=0}_{X_{k+1}|Y_k}(\eta c^T). \tag{37}$$

It has the same functional form as (30) and does not depend on u_k: the dependence of $\bar{\phi}_{S_{k+1}|Y_k}(\eta)$ on u_k is conveniently gathered in the exponential term of (36). Substituting (36) into (34) yields

$$\bar{J}_k(u_k) = \frac{1}{\pi}\int_{-\infty}^{\infty} \frac{\sin(L\eta)}{\eta}\bar{\phi}^{u_k=0}_{S_{k+1}|Y_k}(\eta)\cdot e^{j(c\Lambda)u_k\eta}\mathrm{d}\eta. \tag{38}$$

Similarly to (24), the integral in (38) is solved analytically using the factored form of $\bar{\phi}^{u_k=0}_{S_{k+1}|Y_k}(\eta)$, given in (30), to yield [18]

$$\bar{J}_k(u_k) = \frac{1}{\pi}\sum_{i=1}^{n_t^{k|k}} \left\{ \frac{d_i}{2} \ln \frac{(L-(c\Lambda)\,u_k-\sigma_i)^2+\omega_i^2}{(-L-(c\Lambda)\,u_k-\sigma_i)^2+\omega_i^2} + c_i \left[\arctan\left(\frac{L-(c\Lambda)\,u_k-\sigma_i}{\omega_i}\right) - \arctan\left(\frac{-L-(c\Lambda)\,u_k-\sigma_i}{\omega_i}\right)\right]\right\}, \tag{39}$$

which is the generalized form of (24) for the vector-state case. For simplicity, in (39) the time indices $(k+1|k)$ were removed from the parameters of the characteristic function.

The cost in (39) is a highly nonlinear function of the optimization parameter u_k, and hence is determined using the numerical procedure outlined in Sect. 4.1. Once the optimal u_k^* is determined, it is used as an input to the system and to compute the actual time propagated $\bar{\phi}_{X_{k+1}|Y_k}(\nu)$.

The controller computation steps and its closed-loop implementation is summarized as a flowchart presented in Fig. 2. At any time step k, after obtaining the measurement z_k, first we calculate the measurement updated cf-unpdf $\bar{\phi}_{X_k|Y_k}(\nu)$ using the analytical relations given in [10]. Note that, using the same method, a multi-output system can be handled by processing each component of a vector-valued z_k sequentially. Setting $u_k = 0$, $\bar{\phi}_{X_k|Y_k}(\nu)$ is used to compute the time-propagated cf $\bar{\phi}^{u_k=0}_{X_{k+1}|Y_k}(\nu)$. The time-propagation equations are detailed in [10]. $\bar{\phi}^{u_k=0}_{X_{k+1}|Y_k}(\nu)$ is then used in (37) to determine $\bar{\phi}^{u_k=0}_{S_{k+1}|Y_k}(\eta)$ in the functional form given in (30) and (31). The MCPC control signal, u_k^*, is calculated by maximizing (39). It is applied to the system as well as used to determine the time-propagated cf $\bar{\phi}_{X_{k+1}|Y_k}(\nu)$ through the relations given in [10]. The procedure is repeated when a new measurement is obtained.

In the next section, the proposed MCPC controller is evaluated using a numerical example of a first- and second-order system and its performance is compared to the OPC controller and a Gaussian approximation.

5 Numerical Simulation Results

In this section, the performance of the proposed controller is evaluated using a numerical simulation and compared to the performance of an alternative OPC method[4] and a Gaussian approximation, LEG, both fully discussed in [6] and [7]. First, in Sect. 5.1, the control signal at the first time step is evaluated as a function of the first measurement for a scalar-state system with different parameters. This reveals some important characteristics of the proposed control method. Then, the time response characteristics of a two-state system regulated by the three evaluated controllers are compared in

[4] In [7] this controller is referred to as Cauchy MPC.

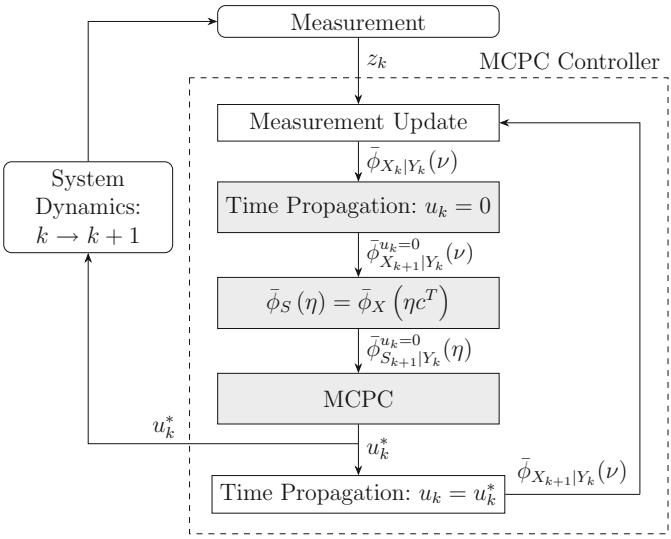

Fig. 2 Flowchart of the controlled system: rounded blocks represent the system; in the MCPC controller, the newly introduced components are marked in grey

Sect. 5.2. Both stable and unstable open loops dynamics are examined here. In these comparisons, for the OPC and LEG controllers we used the same methods, codes and data as in [7].

5.1 First Time Step Control

To better understand the underlying characteristics of the proposed controller, we explore first the optimal control value u_1^* as a function of the first measurement z_1 for a scalar-state system. We consider a system with parameters $\Phi = 0.9$, $H = 1$, $\bar{x}_1 = 0$, $\alpha = 0.1$, $\beta = 0.02$, and $\gamma = 0.5$, and control design parameter $L = 1.5$. In each of the following case studies, we vary one of the scaling parameters γ, β or α around their nominal values. Variations in these parameters change the shape of the associated pdfs and, hence, the shape of the time propagated $f_{X_2|Z_1}(x_2|z_1)$. Consequently, they affect the optimal u_1^*. However, variation in L of $\pm 50\%$ had a minor effect on the numerical results.

Figure 3a depicts the optimal control signal u_1^* versus z_1 for fixed $\alpha = 0.1$ and $\beta = 0.02$, and different values of γ. Not surprisingly, the plot is antisymmetric around $z_1 = 0$. Moreover, it clearly shows the nonlinearity of u_1^* as a function of z_1, except for a nearly linear relation for small $|z_1|$ values. As expected, the slope of the curves around the origin is larger for smaller values of γ, which correctly corresponds to (approximately) higher controller gain for noises with a smaller scaling parameter. Interestingly, for large values of $|z_1|$ the optimal control signal tends to zero. This demonstrates the desirable notion that, since for heavy-tail distributed measurement noises, measurement outliers are more likely (than, e.g., for a Gaussian distribution),

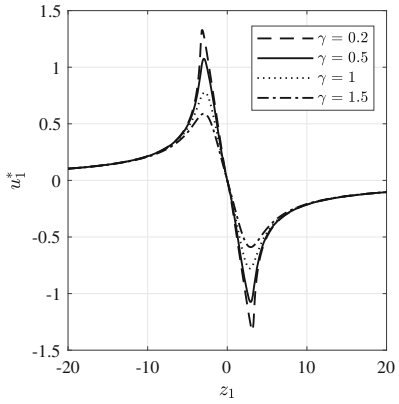

(a) u_1^* vs. z_1 for different γ values.

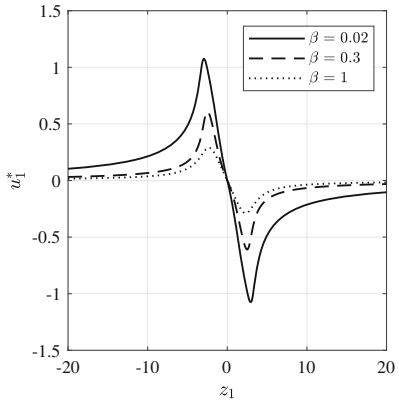

(b) u_1^* vs. z_1 for different β values.

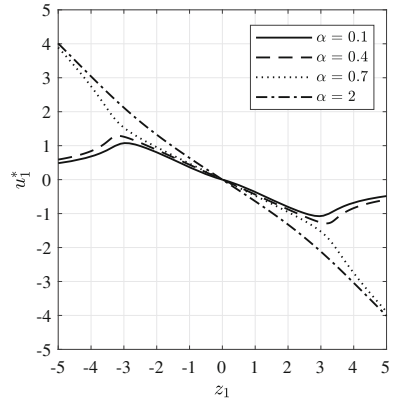

(c) u_1^* vs. z_1 for different α values.

Fig. 3 MCPC control signal u_1^* versus z_1 for different γ, β and α values. Solid line represents the nominal case

a large valued measurement may imply a significant noise component and not a state deviation. Consequently, the control signal u_1^* should be restrained in such cases, as is shown in Fig. 3a.

In Fig. 3b, the optimal control signal u_1^* versus z_1 is shown for fixed $\alpha = 0.1$ and $\gamma = 0.5$, and different scaling parameters β. This plot demonstrates a similar nonlinearity of the control signal as mentioned in the previous paragraph, including the roll-off for high values of $|z_1|$. Here, the control signal is larger for small values of β, indicating that the expected small process noise values will not affect the state at the next time step and, hence, the control action should weigh the current measurement more.

Finally, Fig. 3c presents u_1^* versus z_1 for fixed $\beta = 0.02$ and $\gamma = 0.5$, considering different values of α, the scaling parameter of the pdf of the single initial state x_1. The nonlinear profiles are preserved here for cases that $\alpha < \gamma$. However, when $\alpha > \gamma$ the value of u_1^* is not rolled-off for large $|z_1|$, and the relation between them becomes nearly linear for large α. In those cases, due to the high uncertainty in the initial conditions relative to the measurement uncertainty, the control action relies highly, nearly linearly, on the measurement.

Very similar results of u_1^* versus z_1 were reported for the OPC solution in [6]. This shows the similarity between that and the proposed MCPC approach, which will be further explored in the next subsection addressing the time response characteristics of the various controllers.

5.2 Time Response

The performance of MCPC is compared next against the OPC and LEG controllers derived and discussed in [7]. Here we evaluate the controllers for two second-order systems for which a fixed window approximation for the needed cfs is readily available [23], thus further reducing the simulation run time. Nonetheless, it is important to state that the proposed method is valid for any state dimension.

In this analysis, we evaluate the performance of the three controllers in two cases, characterized by the stability of the controlled system. The first case addresses a stable open loop system given by

$$x_{k+1} = \overbrace{\begin{bmatrix} 0.27 & 0.76 \\ -0.76 & 1.32 \end{bmatrix}}^{\Phi} x_k + \begin{bmatrix} 0.5 \\ 1 \end{bmatrix} u_k + \begin{bmatrix} 0.5 \\ 1 \end{bmatrix} w_k, \tag{40a}$$

$$z_k = [\,1 \quad 1\,]\, x_k + v_k, \tag{40b}$$

with noise parameters $\alpha_1 = \alpha_2 = 0.8$, $\beta = 0.02$ and $\gamma = 0.1$. The eigenvalues of Φ are $\lambda_{1,2} = 0.8 \pm 0.55j$. Their size is $|\lambda_{1,2}| = 0.97$, i.e., Φ is Schur. The sliding variable is chosen such that the closed loop eigenvalues in (10) are $\lambda_1\left(\tilde{\Phi}\right) = 0$ and $\lambda_2\left(\tilde{\Phi}\right) = 0.5$ to yield $c = [\,1 \quad 2.3\,]$. The MCPC controller bound was set to $L = 1.5$.

The second case examined here assumes an unstable system described by

$$x_{k+1} = \overbrace{\begin{bmatrix} -0.16 & 0.81 \\ -1.97 & 1.86 \end{bmatrix}}^{\Phi} x_k + \begin{bmatrix} 0.5 \\ 1 \end{bmatrix} u_k + \begin{bmatrix} 0.5 \\ 1 \end{bmatrix} w_k, \tag{41a}$$

$$z_k = [\,1 \quad 1\,]\, x_k + v_k, \tag{41b}$$

with the same noise parameters. The eigenvalues of Φ in this case are $\lambda_{1,2} = 0.85 \pm 0.76j$. Their size is $|\lambda_{1,2}| = 1.13$, i.e., the system in (41) is unstable. As in the first case, the sliding variable is chosen such that the closed loop eigenvalues in (10) are $\lambda_1\left(\tilde{\Phi}\right) = 0$ and $\lambda_2\left(\tilde{\Phi}\right) = 0.5$. This is obtained by setting $c = [1 \quad 0.4\,]$. The MCPC controller bound was set also to $L = 1.5$.

The simulations results are presented in Figs. 4 and 5. The variables presented are the two states x_1 and x_2, the control signal u, the sliding variable s, and the process and measurement noises w and v.

The first simulation is for a stable open-loop system, presented in Fig. 4. When the process and the measurement noises are relatively small, for example around $k = 40$, MCPC, OPC and LEG controllers behave approximately the same, properly regulating the states around zero. Differences between the three evaluated control schemes can be observed when the system faces large process or measurement noises. Specifically, when a large process noise pulse occurs, for example at $k = 14$, the states deviate from their regulated zero values and the controllers respond, in order to drive them back to regulation. The LEG controller yields a much slower recovery compared to the faster responses when using the MCPC and OPC controllers. Although MCPC is slightly slower in reducing x_1 and slightly faster for x_2, it behaves similarly to OPC.

The difference between the controllers is dramatic when a significant measurement noise is encountered, for example at $k = 53$ in Fig. 4. Being a linear controller, LEG responds immediately, even though the states did not deviate from the zero vicinity, thus unnecessarily exiting the system with corresponding transient error. Surprisingly, the MCPC and OPC controllers correctly ignore the large measurement with a significant noise, therefore maintaining the states near their regulated values.

Very similar performance characteristics are observed also when the open loop system is unstable, as presented in Fig. 5. Again, at $k = 53$ the MCPC and OPC controllers ignore the large measurement with significant noise, whereas the linear LEG controller has even a larger transient error compared to the stable case presented in Fig. 4.

In both stable and unstable cases, it was observed that changing the value of L by up to $\pm 30\%$ has only a minor effect of the performance of the MCPC. This implies that the conditional pdf of the sliding variable is nearly symmetric, and hence L has only a small effect on the optimization in (25).

These results demonstrate clearly that the two controllers designed specifically for Cauchy-distributed process and measurement noises, i.e., OPC and the new MCPC, outperform their Gaussian approximation LEG controller, duplicating the earlier result in [7]. Moreover, examining the time responses, there is no substantial difference between the MCPC and OPC solutions. This demonstrates that in this heavy-tailed

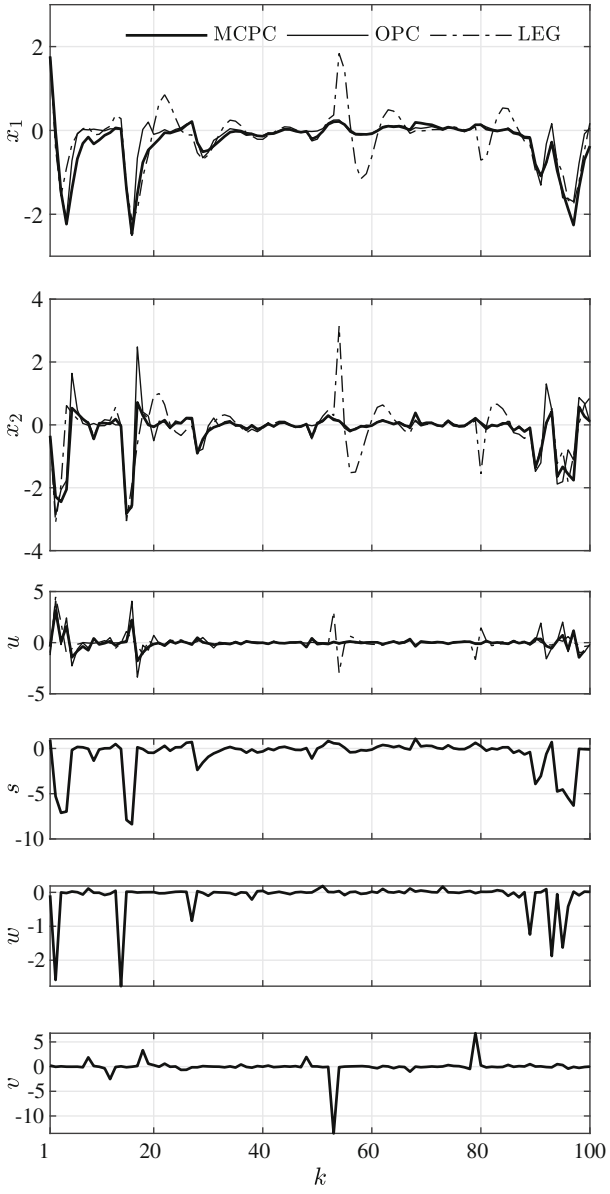

Fig. 4 Regulation performance of the MCPC, OPC, and LEG controllers: stable open loop system

noise environment, at least in the two-state system case examined here, accounting for future systems behavior, as is suggested in OPC, does not enhance performance: a single-step-ahead approach of MCPC yields similar performance with a computationally simpler algorithm. Consequently, the fundamental difference between MCPC and OPC is their computer implementation run time. When tested on the same personal computer and the same software environment (MATLAB), the run time of MCPC was

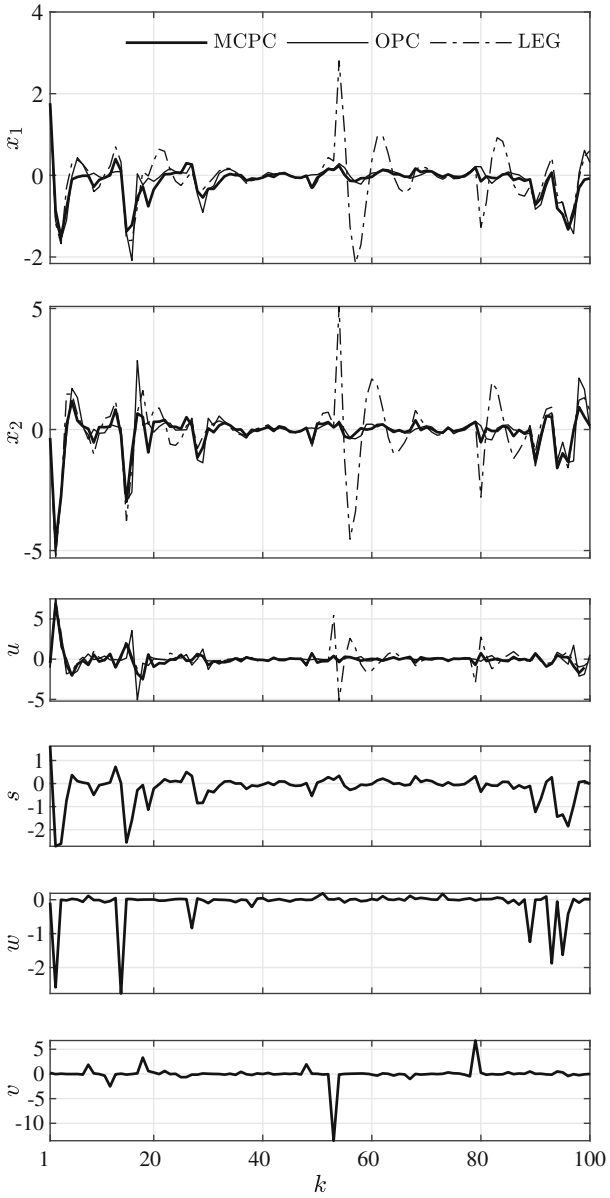

Fig. 5 Regulation performance of the MCPC, OPC, and LEG controllers: unstable open loop system

found to be less than 4% of the time needed to run the OPC. This is of a major importance when considering real-time implementation. The conclusion above should be re-evaluated for higher-order systems. These cases were not addressed in this study because the Cauchy estimator and hence controller implementations suffer from high numerical complexity, which are now being resolved.

6 Conclusions

A new control strategy has been developed for discrete-time, vector-state linear systems driven by Cauchy-distributed process and measurement noises. The motivation for addressing this type of problems is that controllers based on the commonly used light-tailed Gaussian distribution assumption cannot properly capture the dynamic behavior of systems facing extreme process noise inputs and measurement noise outliers. The heavy-tailed Cauchy distribution was found to better represent such system noises. The challenge, when addressing Cauchy distributions, results from the fact that they have an undefined first moment, and infinite higher moments. Consequently, commonly used control and estimation methods cannot be applied in this case. The proposed control strategy was derived using the principles of the deterministic sliding mode control methodology. Since our system is stochastic and thus continuously forced by unbounded noise input, a sliding mode cannot be attained. Alternatively, in this work we propose a control method that at each time step maximizes the conditional probability of the sliding variable being in a pre-defined bound around the sliding manifold. The performance of the proposed controller was tested numerically and compared to a recently derived optimal predictive controller (OPC) and a Gaussian approximation (LEG). The proposed controller has demonstrated similar performance compared to OPC, while both outperformed the LEG controller. The main advantage of the proposed MCPC solution compared to OPC is the significantly lower computational burden of MCPC, enhancing real-time implementation.

Acknowledgements This work was supported by the National Science Foundation (NSF) and United States Israel Binational Science Foundation (BSF) joint NSF-BSF ECCS program under Grants Nos. 2015702 and 2019639, and the NSF Grants Nos. 1607502 and 1934467.

References

1. Bryson, A.E., Ho, Y.C.: Applied Optimal Control: Optimization Estimation and Control. CRC Press, USA (1975)
2. Speyer, J.L., Chung, W.H.: Stochastic Processes, Estimation, and Control. SIAM, (2008). https://doi.org/10.1137/1.9780898718591
3. Zhou, K., Doyle, J.C., Glover, K.: Robust and Optimal Control. Prentice Hall, Inc., USA (1996)
4. Reeves, P.: A Non-Gaussian Turbulence Simulation. Technical Report AFFDL-TR-69-67, Air Force Flight Dynamics Laboratory (1969). https://doi.org/10.21236/ad0701735
5. Kuruoglu, E.E., Fitzgerald, W.J., Rayner, P.J.W.: Near optimal detection of signals in impulsive noise modeled with a symmetric alpha-stable distribution. IEEE Commun. Lett. **2**(10), 282–284 (1998). https://doi.org/10.1109/4234.725224
6. Speyer, J.L., Idan, M., Fernández, J.H.: A stochastic controller for a scalar linear system with additive cauchy noise. Automatica **50**(1), 114–127 (2014). https://doi.org/10.1016/j.automatica.2013.11.005
7. Fernández, J.H., Speyer, J.L., Idan, M.: Stochastic control for linear systems with additive cauchy noises. IEEE Trans. Autom. Control **60**(12), 3373–3378 (2015). https://doi.org/10.1109/tac.2015.2422480
8. Idan, M., Speyer, J.L.: Cauchy estimation for linear scalar systems. IEEE Trans. Autom. Control **55**(6), 1329–1342 (2010). https://doi.org/10.1109/tac.2010.2042009
9. Idan, M., Speyer, J.L.: State estimation for linear scalar dynamic systems with additive cauchy noises: characteristic function approach. SIAM J. Control Optim. **50**(4), 1971–1994 (2012). https://doi.org/10.1137/110831362

10. Idan, M., Speyer, J.L.: Multivariate cauchy estimator with scalar measurement and process noises. SIAM J. Control Optim. **52**(2), 1108–1141 (2014). https://doi.org/10.1137/120891897
11. Aravkin, A.Y., Burke, J.V., Pillonetto, G.: Robust and trend-following student's t Kalman smoothers. SIAM J. Control Optim. **52**(5), 2891–2916 (2014)
12. Bandyopadhyay, B., Janardhanan, S.: Discrete-Time Sliding Mode Control: a Multirate Output Feedback Approach, vol. 323. Springer Science and Business Media, (2005). https://doi.org/10.1007/11524083
13. Shtessel, Y., Edwards, C., Fridman, L., Levant, A.: Sliding Mode Control and Observation. Springer, New York (2014). https://doi.org/10.1007/978-0-8176-4893-0
14. Drakunov, S.V., Su, W.C., Özgüner, U.: Discrete-Time Sliding-Mode in Stochastic Systems. In: Proceedings of American Control Conference (ACC) (1993)
15. Zheng, F., Cheng, M., Gao, W.B.: Variable structure control of stochastic systems. Syst. Control Lett. **22**(3), 209–222 (1994). https://doi.org/10.1016/0167-6911(94)90015-9
16. Poznyak, A.S.: Sliding mode control in stochastic continuos-time systems: μ-zone MS-convergence. IEEE Trans. Autom. Control **62**(2), 863–868 (2017). https://doi.org/10.1109/tac.2016.2557759
17. Twito, N., Idan, M., Speyer, J.L.: Maximum Conditional Probability Stochastic Controller for Scalar Linear Systems with Additive Cauchy Noises. In: 2018 European Control Conference (ECC 18) (2018)
18. Gradshteyn, I.S., Ryzhik, I.M.: Table of Integrals, Series, and Products. Elsevier, Netherlands (2014). https://doi.org/10.1016/c2010-0-64839-5
19. Lagarias, J.C., Reeds, J.A., Wright, M.H., Wright, P.E.: Convergence properties of the nelder-mead simplex method in low dimensions. SIAM J. Optim. **9**(1), 112–147 (1998). https://doi.org/10.1137/s1052623496303470
20. Shephard, N.G.: From characteristic function to distribution function: a simple framework for the theory. Econom. Theory **7**(4), 519–529 (1991)
21. Sasvári, Z.: Multivariate Characteristic and Correlation Functions, De Gruyter Studies in Mathematics, vol. 50. DE GRUYTER (2013). https://doi.org/10.1515/9783110223996
22. Idan, M., Speyer, J.L.: An estimation approach for linear stochastic systems based on characteristic functions. Automatica **78**, 153–162 (2017). https://doi.org/10.1016/j.automatica.2016.12.038
23. Fernández, J.H., Speyer, J.L., Idan, M.: Stochastic estimation for two-state linear dynamic systems with additive cauchy noises. IEEE Trans. Autom. Control **60**(12), 3367–3372 (2015). https://doi.org/10.1109/tac.2015.2422478